

# Measurement of Longitudinal Single-Spin Asymmetry for $W^\pm$ Production in Polarized Proton+Proton Collisions at STAR

**Qinghua Xu, for the STAR collaboration**

Key Laboratory of Particle Physics and Particle Irradiation (MoE), Institute of Frontier and Interdisciplinary Science, Shandong University, Qingdao, Shandong 266237, China

E-mail: xugh@sdu.edu.cn

## **Abstract.**

The contribution from the sea quark polarization to the nucleon spin is an important piece for the complete understanding of the nucleon spin structure. The production of  $W^\pm$  bosons in longitudinally polarized p+p collisions at RHIC provides an unique probe of the sea quark polarization, through the parity-violating single-spin asymmetry,  $A_L$ . At STAR, the  $W$  bosons that decay through the  $W \rightarrow e\nu$  channel at mid-rapidity ( $|\eta| < 1.3$ ) can be effectively determined with the Electromagnetic Calorimeters and Time Projection Chamber. The STAR measurements of  $A_L$  for  $W$  boson from datasets taken in 2011 and 2012 at  $\sqrt{s} = 510$  GeV have been included in the global analysis of polarized parton distribution functions, and provided significant constraints on the helicity distribution functions of  $\bar{u}$  and  $\bar{d}$  quarks. The final  $A_L$  results from 2013 STAR data sample are reported, which is about three times larger than the total integrated luminosity of previous years. The combined results of  $A_L$  for 2011-2013 data are also given. A flavor asymmetry with  $\Delta\bar{u}(x) - \Delta\bar{d}(x) > 0$  is confirmed from a re-weighting of NNPDFpol1.1 after including the new  $A_L$  results. In addition, results on the double-spin asymmetries  $A_{LL}$  for  $W^\pm$ , and  $A_L$  for  $Z/\gamma^*$  production are also reported.

## **1. Introduction**

The contribution from the sea quark polarization to the nucleon spin has been an important piece for a complete understanding of the nucleon spin structure [1]. The knowledge of the sea quark helicity distribution mostly came from the semi-inclusive Deep-Inelastic-Scattering (DIS) process, with still rather large uncertainty [2]. The production of  $W^{+(-)}$  bosons in  $p + p$  collisions with one beam longitudinally polarized provides an unique probe of the sea quark helicity distributions without the involvement of hadron fragmentation as in the semi-inclusive DIS process [3, 4, 5]. In detail, the quantity to be measured at RHIC is the longitudinal single-spin asymmetry  $A_L$  for  $W$  boson production in  $p + p$  collisions, which is defined as:

$$A_L \equiv \frac{\sigma_+ - \sigma_-}{\sigma_+ + \sigma_-} \quad (1)$$

where  $\sigma_\pm$  is the  $W$  cross section with a helicity positive/negative proton beam, with subscripts “ $\pm$ ” here denoting the helicity. The above  $A_L$  equation for  $W^\pm$  can be rewritten as follows at

leading order:

$$A_L^{W^+} = \frac{-\Delta u(x_1)\bar{d}(x_2) + \Delta\bar{d}(x_1)u(x_2)}{u(x_1)\bar{d}(x_2) + \bar{d}(x_1)u(x_2)}, \quad (2)$$

$$A_L^{W^-} = \frac{-\Delta d(x_1)\bar{u}(x_2) + \Delta\bar{u}(x_1)d(x_2)}{d(x_1)\bar{u}(x_2) + \bar{u}(x_1)d(x_2)}. \quad (3)$$

$A_L^{W^+}$  approaches  $\Delta\bar{d}/\bar{d}$  when  $y_W \ll 0$ , since the valence quark usually carries a much larger momentum fraction than a sea quark, and the  $W$  rapidity along the polarized proton beam is defined as positive. Similarly,  $A_L^{W^-}$  approaches  $\Delta\bar{u}/\bar{u}$  when  $y_W \ll 0$ .

In this contribution, we report the final results on the single-spin asymmetries for  $W^\pm$  bosons in longitudinally-polarized  $p+p$  collisions at  $\sqrt{s} = 510$  GeV from the STAR experiment [6]. The data were recorded in 2013 by STAR and correspond to an integrated luminosity of about 250 pb<sup>-1</sup> with an average beam polarization of about 56%, which is about 3 times the previous data sample taken in 2011 and 2012 [7], and thus the most precise measurement of  $W$   $A_L$  at RHIC.

## 2. Experiment and analysis

At the STAR experiment, the  $W \rightarrow e\nu$  events are characterized by an isolated  $e^\pm$  with a sizable transverse energy,  $E_T^e$ , deposited in the Electromagnetic Calorimeter, which peaks near half the  $W$  mass. The neutrino from  $W$  decay is undetected, which leads to a large missing transverse energy that appears as an imbalance in the  $p_T$  sum of all the reconstructed final state particles. In contrast, the  $p_T$  vector is well balanced for background events such as  $Z/\gamma^* \rightarrow e^+e^-$  and QCD di-jet or multi-jet events. The key selection cuts for  $W$  signals are thus based on the lepton isolation and  $p_T$  imbalance features. The charge separation is done using the Time Projection Chamber (TPC), which covers the full azimuth and a pseudorapidity range of  $-1.3 < \eta < 1.3$ . The Barrel and Endcap Electromagnetic Calorimeters (BEMC and EEMC) cover full azimuth and pseudorapidity ranges of  $-1 < \eta < 1$  and  $1.1 < \eta < 2.0$  respectively.

A charged track with high transverse momentum ( $p_T > 10$  GeV/c) is first chosen, then an EMC energy cluster is reconstructed from  $2 \times 2$  calorimeter towers pointed to by the extrapolated track. The cluster energy  $E_T^{2 \times 2}$  in these towers is assigned to the candidate electron. Then, further stages of isolation cuts are implemented, with slight differences between BEMC and EEMC regions. The transverse energy ratio in this  $2 \times 2$  cluster over a surrounding  $4 \times 4$  cluster is required to be larger than 95% (96%) in the BEMC (EEMC) region. It is further required that the candidate electron carry a large fraction (larger than 88% for both BEMC and EEMC) of the energy in the near-side cone with radius  $\Delta R = 0.7$ , where  $\Delta R = \sqrt{\Delta\phi^2 + \Delta\eta^2}$ . After that, a  $p_T$ -balance variable is calculated in terms of the  $p_T$  sum of the electron candidate and the reconstructed jets outside an isolation cone around the electron track with a radius  $\Delta R = 0.7$ . The projection of  $p_T$ -balance to the direction of the candidate electron (named “signed  $p_T$ -balance”), is required to be larger than 14 GeV/c (20 GeV/c) for the BEMC (EEMC) region. In addition, the total transverse energy in the azimuthally away side is required to be less than 11 GeV to further suppress di-jet backgrounds in the BEMC region when one jet loses a sizable fraction of momentum due to detector effects. For the EEMC region, another isolation ratio from the energy deposit in the EEMC shower maximum detector (ESMD) is also used ( $R_{ESMD} > 0.7$ ) [6]. The  $W^\pm$  yield versus the  $e^\pm$  transverse energy  $E_T$  is shown in Fig. 1 with black histograms for different pseudorapidity intervals covered by the BEMC.

There are several contributions to the residual background events under the  $W$  signal peak, as shown in Fig. 1. A QCD di-jet event with one high  $p_T$  lepton can have one of its jets outside the STAR acceptance and thus pass all the  $W$  selection criteria. Such events will be accepted if the detected jet or electron passes all the above  $W$  selection criteria, which is referred as “QCD background”. Also, the  $Z/\gamma^* \rightarrow e^+e^-$  event with one of electron/positron outside the STAR acceptance is another source of the residual background. In addition, the  $W$  boson can decay

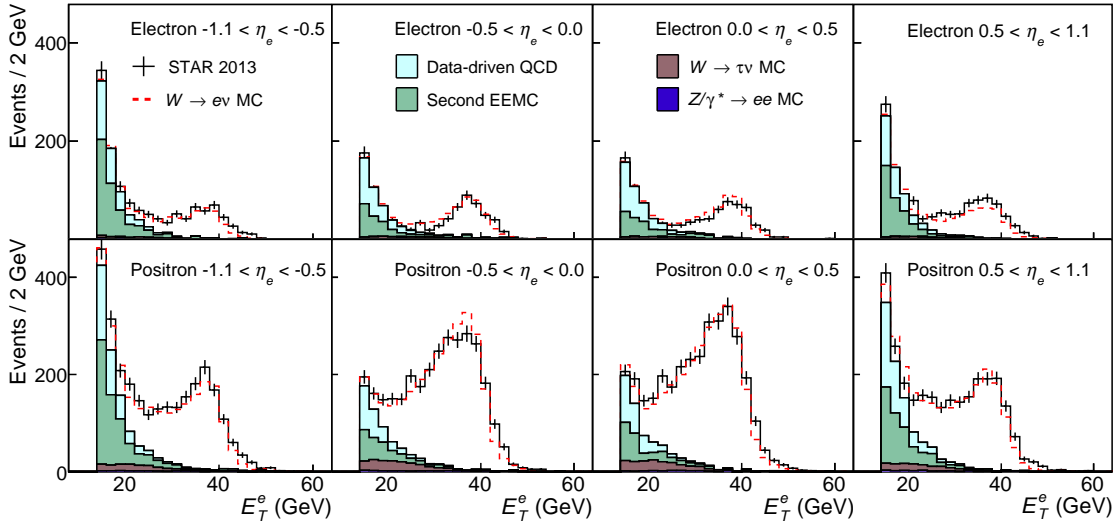


**Figure 1.**  $E_T^e$  distribution for  $W^-$  (top) and  $W^+$  (bottom) candidates (black), background contributions, and the sum of background and  $W \rightarrow e + \nu_e$  Monte Carlo (MC) signals (red dashed) from STAR 2013 data [6].

to  $\tau + \nu$  and  $\tau$  can further decay to an electron and a neutrino, though we will not distinguish this feed down contribution. The  $Z/\gamma^*$  and  $\tau$  contributions are estimated with MC events generated using PYTHIA [8] that pass through the STAR simulation framework and then are embedded into zero-bias  $p+p$  events. The QCD background is first estimated using the existing EEMC detector for the uninstrumented acceptance region on the opposite side of the collision point and the rest is estimated using a data-driven method [7]. In Fig. 1, different background contributions mentioned above are shown as the colored histograms. The residual background fraction is found to be a few percent and is corrected in the determination of the single-spin asymmetry for  $W$  signals, as detailed in Refs. [6, 7].

### 3. Results and discussion

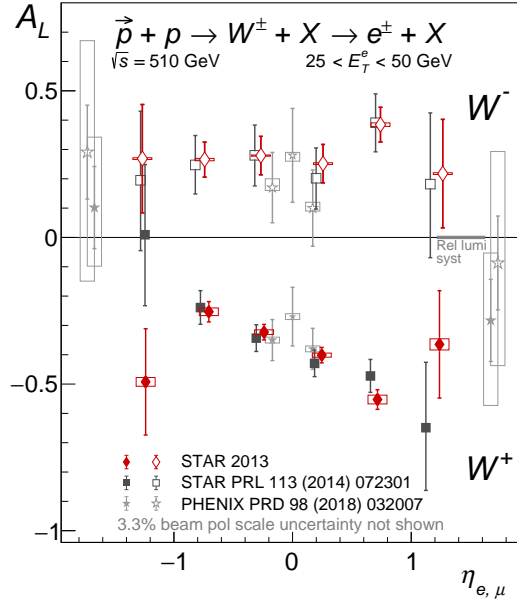
The longitudinal single-spin asymmetry  $A_L$  for the combination in which the first beam is polarized and the second carries zero net polarization is determined from:

$$A_L = \frac{1}{\beta P} \frac{R_{++}N_{++} + R_{+-}N_{+-} - R_{-+}N_{-+} - R_{--}N_{--}}{R_{++}N_{++} + R_{+-}N_{+-} + R_{-+}N_{-+} + R_{--}N_{--}} \quad (4)$$

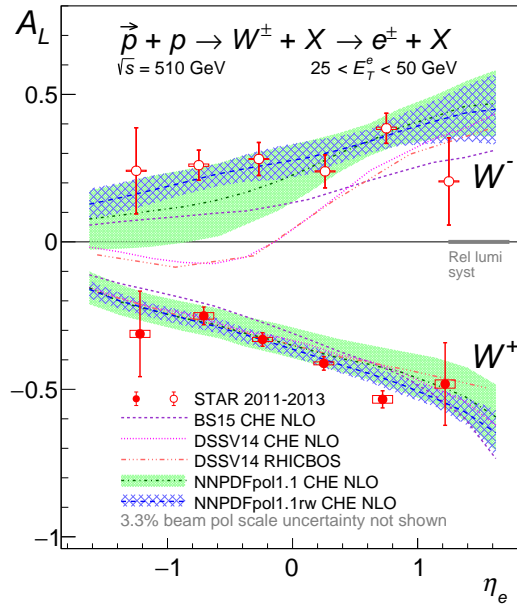
where  $\beta$  is the signal purity,  $P$  is the average beam polarization, and  $R$  and  $N$  are the normalizations for relative luminosity and the raw  $W^\pm$  yields with  $25 < E_T^e < 50$  GeV, respectively, for the helicity configurations indicated by the subscripts. The relative luminosities are obtained from a large QCD sample that exhibits no significant single-spin asymmetry.

Figure 2 shows the final  $A_L$  results for  $W^\pm$  boson versus lepton pseudorapidity from the STAR 2013 data sample [6], in comparison with STAR results from the 2011+2012 data [7] and the final PHENIX results of  $A_L$  for leptons from  $W/Z$  decay [9, 10]. The systematic uncertainties are indicated by open boxes. The STAR 2013  $A_L$  results are consistent with the previous STAR 2011+2012 results, with 40 – 50% smaller statistical uncertainties.

The combined STAR data from years 2011-2013 are shown in Fig. 3, in comparison with theoretical expectations based on the NNPDFpol1.1 [11], DSSV14 [12] and BS15 [13] global analyses under the next-to-leading order CHE [14] and fully resummed RHICBOS [15]



**Figure 2.** Single-spin asymmetry  $A_L$  for  $W^\pm$  production as a function of  $\eta_e$  in  $p + p$  collisions at 510 GeV from STAR 2013 data [6], in comparison to STAR 2011+2012 data [7] and the PHENIX data [9, 10].



**Figure 3.** Longitudinal single-spin asymmetries,  $A_L$ , for  $W^\pm$  production as a function of  $\eta_e$ , for the combined 2011+2012 and 2013 STAR data samples [6] in comparison to theory expectations.

frameworks. The NNPDFpol1.1 expectation includes the STAR  $A_L$  results from 2011 and 2012 data [7], while DSSV14 and BS15 do not. The STAR 2013  $W$   $A_L$  results have reached unprecedented precision and will significantly advance our understanding of the nucleon spin structure in particular the sea quark polarization. To assess their impact, the STAR 2013 data were used in the reweighting procedure of NNPDF global fit based on NNPDFpol1.1

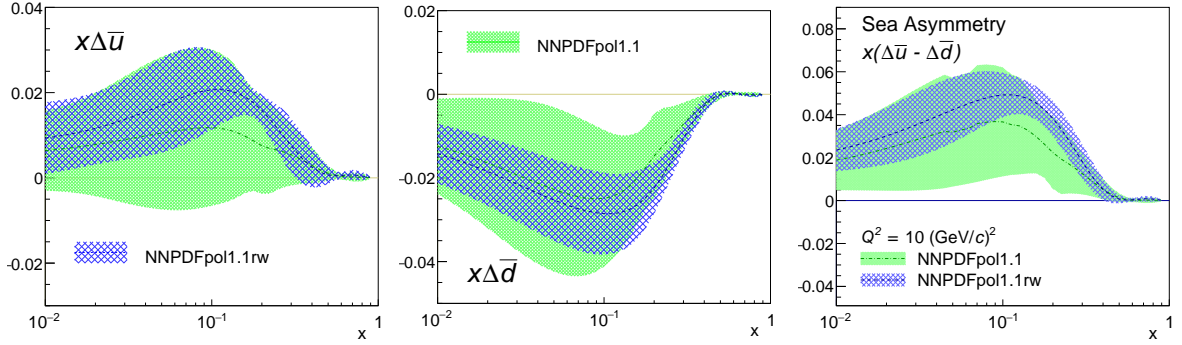


**Figure 4.** The helicity distributions of  $\bar{u}$  and  $\bar{d}$  and their difference  $\Delta\bar{u} - \Delta\bar{d}$  as a function of  $x$  at a scale of  $Q^2 = 10 (\text{GeV}/c)^2$ . The green curve/band shows the NNPDFpol1.1 result [11] and the blue curve/band shows the corresponding distribution after the 2013  $W^\pm$  data are included by reweighting [6].

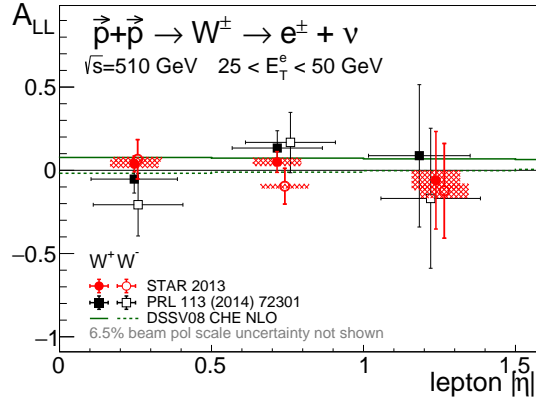


**Figure 5.** Longitudinal double-spin asymmetries,  $A_{LL}$ , for  $W^\pm$  production as a function of  $\eta_e$ , for the 2013 STAR data samples [6] in comparison to theory expectations.

parton densities [11]. The results from the reweighting are shown in Fig. 3 as the blue hatched bands, which are significantly reduced compared the bands before the reweighting. The helicity distributions of  $\bar{u}$  and  $\bar{d}$  in the proton from the reweighting and their difference  $\Delta\bar{u} - \Delta\bar{d}$  are shown in Fig. 4 [6]. The new STAR data now confirm the existence of a flavor asymmetry in the polarized quark sea,  $\Delta\bar{u}(x) > 0 > \Delta\bar{d}(x)$ , in the range of  $0.05 < x < 0.25$  at a scale of  $Q^2 = 10 (\text{GeV}/c)^2$ . This is opposite to the flavor asymmetry observed in the unpolarized quark distributions, where  $\bar{d}(x) > \bar{u}(x)$  over a wide  $x$  range has been observed [1].

Other than  $W^\pm$ ,  $A_L$  is also determined for  $Z/\gamma^*$  production from a sample of 274  $Z/\gamma^*$  candidates with electron–positron pair invariant mass  $70 < m_{e^+e^-} < 110 \text{ GeV}/c^2$  from STAR 2013 data. The residual background is negligible. The measured result,  $A_L^{Z/\gamma^*} = -0.04 \pm 0.07$  with negligible systematic uncertainty, is consistent with theoretical expectations,  $A_L^{Z/\gamma^*} = -0.08$  from DSSV14 [12] and  $A_L^{Z/\gamma^*} = -0.04$  from NNPDFpol1.1 [11].

In addition, we also measured the longitudinal double-spin asymmetry  $A_{LL} \equiv (\sigma_{++} + \sigma_{--} - \sigma_{+-} - \sigma_{-+}) / (\sigma_{++} + \sigma_{--} + \sigma_{+-} + \sigma_{-+})$ , which can provide additional constraints on the  $\Delta\bar{u}(x)$  and  $\Delta\bar{d}(x)$  distributions. The results of  $A_{LL}$  for  $W^\pm$  are shown in Fig. 5, and compared with theory expectations.

#### 4. Summary

In summary, we report new STAR measurements of the longitudinal single-spin asymmetry for  $W^\pm$  bosons produced in polarized proton+proton collisions at  $\sqrt{s} = 510$  GeV. The production of weak bosons provides a unique probe of the sea quark helicity distribution functions of the proton. The new  $A_L$  results, with highest precision at RHIC, show a significant preference for  $\Delta\bar{u}(x) > 0 > \Delta\bar{d}(x)$  in the fractional momentum range  $0.05 < x < 0.25$  at  $Q^2 \sim 10$  (GeV/c) $^2$ .

The author is supported partially by the Natural Science Foundation of China (No. 11520101004) and the Major State Basic Research Development Program in China (No. 2014CB845400).

#### References

- [1] See for example, W. C. Chang and J. C. Peng, *Prog. Part. Nucl. Phys.* **79**, 95 (2014).
- [2] See for example, D. de Florian, R. Sassot, M. Stratmann and W. Vogelsang, *Phys. Rev. D* **80**, 034030 (2009).
- [3] C. Bourrely, J. Soffer, *Phys. Lett. B* **314**,132(1993).
- [4] G. Bunce, N. Saito, J. Soffer, and W. Vogelsang, *Ann. Rev. Nucl. Par. Sci.* **50**, 525 (2000).
- [5] F. Tian, C. Gong, B.-Q. Ma, *Nucl. Phys. A* **961**, 154(2017);  
M.Y. Liu, B. -Q. Ma, *Phys. Rev. D* **98**, 036024 (2018).
- [6] J. Adam *et al.* [STAR Collaboration], *Phys. Rev. D* **99**, 051102R (2019).
- [7] L. Adamczyk *et al.* [STAR Collaboration], *Phys. Rev. Lett.* **113**, 072301 (2014).
- [8] T. Sjostrand, S. Mrenna, and P. Skands, *JHEP* **05**, 026(2006).
- [9] A. Adare *et al.* [PHENIX Collaboration], *Phys. Rev. D* **93**, 051103 (2016).
- [10] A. Adare *et al.* [PHENIX Collaboration], *Phys. Rev. D* **98**, 032007 (2018).
- [11] E. R. Nocera *et al.* [NNPDF Collaboration], *Nucl. Phys. B* **887**, 276 (2014).
- [12] D. de Florian, R. Sassot, M. Stratmann and W. Vogelsang, *Phys. Rev. Lett.* **113**, 012001 (2014).
- [13] C. Bourrely and J. Soffer, *Nucl. Phys. A***941**, 307(2015).
- [14] D. de Florian and W. Vogelsang, *Phys. Rev. D* **81**, 094020 (2010).
- [15] P.M. Nadolsky and C.P. Yuan, *Nucl. Phys.* **B666**, 31(2003).